Postprint of: Grzesiak W., Mackow P., Maj T., Polak A., Klugmann-Radziemska E., Zawora Sz., Drabczyk K., Gulkowski S., Grzesiak P., Innovative system for energy collection and management integrated within a photovoltaic module, Solar Energy, Vol. 132 (2016), pp. 442-452, DOI: 10.1016/j.solener.2016.03.043

Innovative system for energy collection and management integrated within a photovoltaic module

Wojciech Grzesiak,[1] Piotr Mackow,[1] Tomasz Maj,[1] Artur Polak,[1]

Ewa Klugmann-Radziemska,[2] Szymon Zawora,[3] Kazimierz Drabczyk,[4]

Slawomir Gulkowski,[5] Paweł Grzesiak[6]

[1] Institute of Electron Technology – Krakow Division, 39 Zablocie St., 30-701 Krakow, Poland. Tel. +48126563144, fax. +48126563626, email: grzesiak@ite.waw.pl
[2] Gdańsk University of Technology, Chemical Faculty, 11/12 Narutowicza St., 80-233 Gdansk, Poland
[3] Zamel Ltd, 27 Zielona St., 43-200 Pszczyna, Poland
[4] Institute of Metallurgy and Materials Science of Polish Academy of Sciences, 25 Reymonta St., 30-059 Krakow, Poland
[5] Lublin University of Technology, 38 Nadbystrzycka St., 20-618 Lublin, Poland
[6] University of Economics in Krakow, 27 Rakowicka St., 31-510 Krakow, Poland

Abstract

The dynamic development of battery technology and design based on the flow of lithium ions, which is mainly driven by the needs of the automotive industry, leads to the conclusion that these batteries are becoming a more viable alternative to traditional lead-acid batteries. Their use is driven by their ability to charge and discharge quickly, higher durability, maintenance-free operation, much smaller dimensions, and lighter weight. The emergence of super-thin $LiFePO_4$ battery technology inspired the design and implementation of a prototype of a portable photovoltaic module that is integrated with the battery and an innovative system for data gathering and power management. This paper presents a block diagram of a prototype and discusses issues related to the selection of components and the design and implementation of individual blocks. In particular, it considers an innovative system that quickly and accurately supports the elevation and declination angle of the module and the system for monitoring the state of battery charge and discharge.

Basic technical parameters are described, as well as the possibility of scaling up the system. Mechanical construction details, the concept of research stations, and the results obtained during the research are presented. An analysis of the areas of application and economic aspects of the solution are also taken into consideration.

Keywords: stand-alone photovoltaic system, data gathering and power management, integrated battery, super-thin $LiFePO_4$ battery, charge/discharge controller, battery status monitor

Introduction

The worldwide growth of photovoltaics (PV) has followed an exponential curve for more than two decades. During this period, PV has evolved from a pure niche market of small-scale applications towards becoming a mainstream electricity source. Regardless of the global trend of attaching large installations to the grid, off-grid electrification is still the main approach to accessing electricity in countries and areas with little access to electricity.

The term “off-the-grid” can refer to living in a self-sufficient manner without relying on one or more public utilities. Decentralized electricity production, defined as electricity-based production within a village that is not linked to a grid or to transmission or distribution networks, provides a plausible medium-term solution to the electricity accessibility issue in some countries that are suited to solar energy (for example, India and Nigeria). According to the IEA (2009), 1.456 billion people worldwide (18% of the world's population) do not have access to electricity, and 83% of these people live in rural areas.

The availability of energy is an important pre-condition for developing the national economy and improving the living standards of people. The application of PV-based home electrification will offer a quick, economic, and reliable answer to the need for power in rural households, especially those using light-duty appliances.

Therefore, there needs to be an assessment of the potential of a solar PV-based rural home electrification project that will meet the basic energy needs of rural homes without increasing stress on the power grid.

The domestic load demand of rural areas, which will serve as input data in the design of PV-based rural home electrification systems and also assist governments in their rural electrification planning framework, has been assessed. For example, rural households in Nigeria will require 850.8 kWh/yr to meet their basic power requirements for loads such as lighting and electronic appliances (for example, radios and televisions) [1]. The governments of these countries recommend that solar PV-based rural home electrification applications should be encouraged.

In most rural regions, villages are located 3 to 80 km (or even further) away from the existing grid in difficult areas like forests, hills, and deserts. The number of households in a village may range between 2 and 200 with a dispersed distribution of loads. The power demand of villages is quite low, and rural domestic consumers are mainly peak-time consumers who contribute low load factors of 0.2–0.3 [2].

Stand-alone PV systems can be implemented with single components or assembled and integrated by the manufacturer. A kit of this kind is often called a ‘solar home station’. A solar home station is a portable kit designed specially to meet basic domestic power requirements in grid-isolated, high-temperature regions of the world. Elements of such autonomous systems are a PV module or modules, an electronic controller, and battery charging. The nominal voltage of the system battery in such a kit is usually 12, 24, or, less frequently, 48 V. In cases where the installation provides power to consumers, which requires alternating voltages of 110 or 230 V, an appropriate electronic DC/AC converter is required. Typical home appliances that can be powered by the system are colour TV, radio, lighting,

computers, mobile phones, and ventilation (fans). It can also be the source of electric power for military applications, security signalling and lighting, and charging mobile phones. There are many examples of such systems offered by manufacturers.

Figure 1 shows an example of such a system designed and built by the German company Solar Fabrik AG (left) [3], as well as one built by the Institute of Electron Technology Division in Krakow, commissioned by Sunflower Farm (right).

As the solar market grows worldwide, the importance of implementing deep-cycle batteries as the energy storage component for renewable energy systems is critical. These systems are typically based on so-called "long life" lead-acid solar batteries; they are therefore bulky and have a limited lifespan of typically five years. The first problem that must be faced is reducing the size and weight of the system. The second one is extending the lifetime of the energy accumulator in order to bring it closer to the lifetime of the PV module. In addition to their degradation capacity, lead-acid batteries are characterized by large dimensions and a low resistance to freezing temperatures. These shortcomings have led to increased interest in lithium-ion technology in PV installations. Simultaneously, a significant reduction in prices is projected due to the effect of increasing the scale of production, which is likely to translate into achieving a market advantage over storage solutions based on lead-acid technologies.

Unlike lead-acid technology, lithium-ion batteries have a much longer life span. After about 500 charge/discharge cycles, cyclic-operation standard gel batteries show a significant reduction in capacity; under the same conditions, lithium-iron-phosphate ($LiFePO_4$) batteries withstand about 3,000 charge/discharge cycles. The lifetime of such a lithium-ion battery is much closer to the lifetime of a PV module and electronic controller, which will allow a commercial device with high cumulative stability to be offered in the future. The big advantage here is the possibility of $LiFePO_4$ batteries charging and discharging large currents

of the order of 1 C, while lead-acid batteries can operate at currents of up to 0.3 C. The main disadvantage of lithium-ion technology is its sensitivity to the conditions of charging and discharging processes, which can lead to significant degradation of battery capacity and, eventually, destruction of the battery. Unlike lead-acid batteries, rechargeable batteries based on $LiFePO_4$ technologies require the use of the electronic management system.

The primary objective of the scheme is to equalize the charge level of cells in the package (in the process of both charge and discharge cycles), to measure temperature and prevent the battery from exceeding its temperature limit, and often also to monitor and inspect the discharge process. These systems may be based on dedicated integrated circuits, which are offered by most leading manufacturers.

The third problem to be solved is the partial shading of the PV module. The reduction in power output caused by the accumulation of dust on the PV module surface is an important problem. Dust is created from powdered grains of sand and particles of different bodies. Dust originates from different sources, for example from soil and volcanic eruptions. Dust in the air is an aerosol and, in high concentrations, can cause climate change. The deposition of airborne dust on PV modules may decrease the transmittance of solar cell glazing and cause a significant degradation in the solar conversion efficiency of PV modules. Many researchers have devoted their work to studying the origin, composition, and gradation of dust grains originating from different regions of the world [4]–[7] and their influence on PV module performance.

Materials and Methods

A PV module integrated with an accumulator and an innovative system for data gathering and power management was built on the basis of the block diagram illustrated in Figure 2.

Figure 3 presents details of the construction of the PV module integrated with the accumulator and innovative system for gathering and power management.

PHOTOVOLTAIC MODULE

The basic element of the structure is the monocrystalline PV module, RS 36-125*125M-100, which has dimensions of 1193 mm × 539 mm × 25 mm, weighs 7.6 kg, and is manufactured by Risen Energy Co. It has a nominal power of 100 W, open voltage of V_{oc} = 22.8 V, and short circuit current of I_{sc} = 6.03 A. The voltage at the point of maximum power is V_{MPP} = 18.4 V and the current at the point of maximum power is I_{MPP} = 5.43 A.. The solution allows for a structure with dimensions that do not exceed the dimensions of the PV module.

BATTERY

$LiFePO_4$ batteries are fairly new for solar use. They have no toxic chemicals and offer four times the power density at a third of the volume compared to lead-acid batteries. Laboratory results indicate that 2000 to 5000 cycles can be expected from a well-maintained $LiFePO_4$ battery bank; a battery will still deliver more than 75% of its capacity after 2000 cycles. In contrast, even the best deep cycle lead-acid batteries are typically only good for 500–1000 cycles. $LiFePO_4$ batteries have almost no self-discharge – they can stay disconnected without any problems for 10 months and will still be almost fully charged.

$LiFePo_4$ batteries appear well-suited for off-grid renewable applications. They show not only the least degradation under variable charging protocols, which are characteristic of all types of off-grid renewable energy generation, but also the best voltage performance. Their long lifetime would reduce the frequency of battery replacement of solar systems [8].

We propose that the Nanophosphate® Lithium Ion Prismatic Pouch Cell be combined with the 100 W monocrystalline PV module. Nanophosphate® is a positive electrode material with a remarkable rate capability, which is critical for high power systems. The cell dimensions of a single 19.6 Ah (minimum) cell capacity are equal to 7.25 mm × 160 mm × 227 mm. Four cells connected in series to form a battery with a rated voltage of 13.2 V and a capacity of 20 Ah were used. However, the dimensions of the back cavity of the module even allow the use of a complex battery of 12 cells connected in series and in parallel with a total capacity of 60 Ah. The advantages of Nanophosphate® are its higher charge and discharge rates, which lead to better performance and efficiency, a wide SOC (State of Charge) range, enabling greater battery utilization, superior abuse tolerance, and long battery life for both deep and shallow cycling [9]. Table 1 presents the specifications of the A123 AMP20 battery.

Table 1. AMP20 cell specification [9]

Dimensions [mm]	7.25 × 160 × 227
Mass [g]	496
Capacity (minimum) [Ah]	19.6
Voltage (nominal) [V]	3.3
Energy content (nominal) [Wh]	65
Discharge power (nominal) [W]	1200
Maximum discharge current [A]	100
10 s discharge current [A]	600
Cycles (depth of discharge = 90%)	3000
Operating temperature [°C]	–30 to 55
Storage temperature [°C]	–40 to 60

The system is also equipped with a commercial accumulation-type module, PCM-L04S25-808 12.8/20A for $LiFePO_4$ (4S), to balance the individual cell voltages. This system also protects the cells against overload, excessive discharge, short circuiting, and overheating. The main parameters are summarized in Table 2.

Table 2. Technical parameters of the PCM-L04S25-808 module [10]

Maximal continuous charging current [A]	20
Maximal continuous discharging current [A]	20
Balance current for single cell [mA]	72 ± 10
Balance voltage for single cell [V]	3.6 ± 0.025
Overcharge detection voltage [V]	3.9 ± 0.025
Overcharge release voltage [V] [V]	3.8 ± 0.025
Over-discharge detection voltage [V]	2.0 ± 0.05
Over-discharge release voltage [V]	2.3 ± 0.05
Dimensions [mm]	70 × 60 × 9

BATTERY CHARGE CONTROLLER

The model controller was designed and manufactured based on an LT 8490 dedicated integrated circuit [11]. It was examined by the manufacturer by providing samples and informative materials before placing it on the market. Its schematic diagram is shown in Figure 4; a photograph of it is shown in Figure 5.

Use of the LT 8490 system made it possible to:

- obtain a broad range of input (6–80 V) and output (1.3–80 V) voltages due to an implemented DC/DC buck-boost,

- obtain a very high efficiency,
- search for the real point of maximum power even when the module was partially overridden,
- adapt to the needs of both lead-acid batteries and $LiFePO_4$ by employing a CC/CV (constant current/constant voltage) charging algorithm,
- enable cooperation with other energy sources,
- carry out compensation of the effect of changes in the ambient temperature.

BATTERY DISCHARGE CONTROLLER

A battery discharge controller was developed and manufactured for discharge process management (Figure 6). It protects the battery from deep discharge and from a discharge current that is too high. The protection against a discharge current that is too high takes into account the possibility of temporarily exceeding the maximum permissible discharge current and exceeding the average value of the current in a given period of time.

Of particular note is the use of a commercial, fully integrated Hall-effect-based linear current sensor of type ACS 712 ELCTR-30 A-T, optimized for the measurement of currents up to 30 A with input resistance of 1.2 mΩ and MOSFETs for very a low value of $R_{DS(on)}$ of 1 mΩ, allowing for a substantial reduction of power and preventing waste in the system.

The use of a highly energy-efficient DC/ DC converter of type LT 3970, lowering the voltage to 5 V, and the ability to switch off the current sensor and OLED display allow additional saved energy to be stored in the battery. This is particularly important especially in the final phase of discharge of the battery. The OLED display used had low power consumption and high contrast. Figure 7 shows the manner of displaying the selected parameters.

The use of an ATmega88 microcontroller and the dedicated software allows for the measurement of battery voltage and charge and discharge currents and provides the

opportunity to read them on the OLED display. The observation of changes in the battery charging current makes it possible to choose the optimum elevation angle and declination demonstrator settings. It is possible to set the value of all parameters via RS-232.

It is possible to expand the system with a battery SOC monitor, enabling determination of the amount of energy currently stored in the accumulator, and the function of remote reading of data through the use of a dedicated application for mobile smart phones.

Results

A research station was designed and constructed for the purpose of the experiment. The block diagram is shown in Figure 8.

The following equipment was used for measuring voltages and currents:

- Keithley 2700 digital multimeters with a resolution of 6 1/2 digits, equipped with a Keithley 7700 twenty-channel universal multiplexer card,
- two Keithley 1651 shunts (R1, R2) for an ammeter, 50 A, 0.001 Ohm, ± 1%,
- AgilentE4350B/J03 simulator of PV modules, 10 A, 480 W, with the author's management software and the commercial software Solar Design Studio v6.0,
- BK 8510 programmable electronic load, allowing for the measurement of characteristics of the discharge mode CC, CV, constant power (CP), and constant resistance (CR),
- personal computer (PC),
- type LI-250 pyranometer equipped with an LI200 probe,

To measure the temperature of individual elements of a system, a Thermo-Hunter model BS-02T non-contact thermometer with a measuring range of 0–500 °C and accuracy of ± 1% was used.

Measurements were carried out with the use of an Endeas QuickSUN 820A commercial solar simulator with a manual measuring system. Electrical parameters of the module were determined for the STC (Standard Test Conditions: irradiation = 1000 W/m^2; temperature = 25 °C; radiation spectrum: AM1.5). This type of simulator is a high-performance device equipped with a Xenon flash. It allows for the determination of the full current-voltage characteristics of the module while maintaining the AAA class. This class is determined in accordance with IEC 60904-09, edition 2. The simulator has the appropriate filters for the preservation of the spectrum AM1.5 uniformity and an adequate distribution of radiation over the entire surface of the test module. In addition, the test stand has additional generators that allow for an extension of the duration of the flash so that the parameter LTI (Long Term Instability) complies with the conditions of class A.

The management program is written in Delphi and is designed to work on PCs with Windows XP and later. It enables, via the RS232 interface or USB, the remote management and monitoring of the simulator, electronic load, and multimeter with the scanner. Thanks to this program, any experiment involving charging and discharging the battery and recording voltage as a function of time at the five points of the system can be realized. The system makes it possible to carry out research in real and simulated conditions.

Exemplary results of the characteristics of the RS 36-125*125M-100 module generated by the simulator are shown in Figure 9.

For the examination of the MPP (Maximum Power Point) search accuracy, the simulator was used to generate: 1) the output characteristics of a typical 12 V monocrystalline silicon module for solar irradiation of 100, 200, 400, 600, 800, and 1000 W/m^2 (Figure 10), and 2) the characteristics of the partially overridden module (Figure 11).

The point where the red lines cross shows the precision of the MPP search. The search time is completed within seconds. An analysis of the behaviour of the regulator through the testing of input-output characteristics of the module leads to the conclusion that the system is working properly and in accordance with our expectations. The MPP search is completed in a fast, precise, and correct manner in the case of the partially shaded modules. The behaviour of the system in the case of low solar irradiation of the module surface (100 W/m^2) is also highly promising.

Experimental studies concerning the impact of partial shading of the PV module on the electrical power generated were carried out with the use of the modules produced on the basis of monocrystalline silicon cells of type SF 110 with the following basic parameters: P_{MPP} = 110 W, V_{OC} = 21.6 V, V_{MPP} = 17.4 V, I_{MPP} = 6.32 A, and I_{SC} = 6.76 A. Modules SF 150/10A-155 have the following basic parameters: P_{MPP} = 110W, V_{OC} = 21.6 V, V_{MPP} = 17.4 V, I_{MPP} = 6.32 A, and I_{SC} = 6.76 A. Modules 85S-12B have the following key parameters: P_{MPP} = 85 W, V_{OC} = 22.5 V, V_{MPP} = 17.8 V, I_{MPP} = 4.80 A, and I_{SC} = 5,15 A.

A study of the partially shaded module, with an override of ¼, ½, ¾, 1, and 8 cells, was also conducted. Based on the analysis of the graph in Figure 12 it can be concluded that in the case of the ¼ and ½ shaded cells, the MPP point,, is located in the vicinity of about 0.8–0.9 V_{oc}, while the rest of the points are shifted and occur in the vicinity of 0.5 V_{oc} [12–15]. Based on numerous studies of commercial charging controllers, it was found that most of them cannot find the MPP in the case of an unusual location. To solve this problem, a dedicated controller

chip that was able to find the abnormal locations by searching for locally positioned MPP points was used.

It was possible to measure the characteristics and precise charging time of the battery.

Examples of battery charging characteristics from a PV module simulator for 1000 W/m^2 and a temperature of 25 °C are shown in Figure 13. Solar energy was used to charge the batteries. During charging, the irradiation varied between 800 and 1000 W/m^2; the charging time was approximately 3 hours. The charging process was monitored with the use of a charge controller, and this was continued until the terminal voltage of the battery reached the value of 14.2 ± 0.15 V. The examination of the loading process was initiated with the simulation of typical output characteristics of the PV module of 12 V/150 W.

After charging the battery, the subsequent process of battery discharge was carried out with sequence currents of 5, 10, and 20 A (Figure 14). Discharge times were, successively, 3 hours 50 minutes, 1 hour 54 minutes, and 55 minutes.

Conclusions

The proposed solution is an interesting and much more mobile alternative to a solar home station, which was described in the introduction. It is also planned to further increase the mobility of the implementation of the version shown in Figure 15.

The designed and examined innovative gathering and energy management system integrated within a PV module meets the requirements for stand-alone power stations and tackles the previously identified problems: it is an integrated system with minimized dimensions and weight, allowing for operation with maximum power point control and power settings for an optimal angle of elevation and declination.

Similar results were obtained with PV systems for charging the batteries of electrically powered vehicles, where high system efficiency was achieved by directly charging the battery from the PV system and matching the PV maximum power point voltage to the battery charging voltage at the desired maximum state of charge of the battery [16].

The system can be used for camping, in gardens and allotments, on vessels, in mobile monitoring, warning, and information systems, and so on. It has been registered with the Polish Patent Office under patent no. P.410653 [17].

References

[1] Adeoti O, Oyewole BA, Adegboyega TD. Solar photovoltaic-based home electrification system for rural development in Nigeria: domestic load assessment; Renewable Energy 2001; **24**: 155–161.

[2] Kamalapur GD, Udaykumar RY. Rural electrification in India and feasibility of photovoltaic solar home systems; Electrical Power and Energy Systems 2011; **33**: 594–599.

[3] Solar Home Station Basic – Solar Fabrik AG: Training materials 1999; http://solar-innovation.com/products/homestation.html.

[4] Klugmann-Radziemska E. Degradation of electrical performance of a crystalline photovoltaic module due to dust deposition in northern Poland; Renewable Energy 2015; **78**: 418-426, DOI: 10.1016/j.renene.2015.01.018.

[5] Sarver T, Al-Qaraghuli A, Kazmerski LL. A comprehensive review of the impact of dust on the use of solar energy: History, investigations, results, literature, and

mitigation approaches; Renewable and Sustainable Energy Reviews 2013; **22**: 698–733, DOI:10.1016/j.rser.2012.12.065.

[6] Cabanillas RE, Munguía H. Dust accumulation effect on efficiency of Si photovoltaics modules; Journal of Renewable and Sustainable Energy 2011; **3**: 043114-1-8, DOI: 10.1063/1.3622609.

[7] Beattie NS, Moir RS, Chacko C, Buffoni G, Roberts SH, Pearsall NM. Understanding the effects of sand and dust accumulation on photovoltaic modules; Renewable Energy 2012; **48**: 448–452, DOI:10.1016/j.renene.2012.06.007.

[8] Krieger EM, Cannarella J, Arnold CB. A comparison of lead-acid and lithium-based battery behavior and capacity fade in off-grid renewable charging applications; Energy 2013; **60**: 492–500, DOI:10.1016/j.energy.2013.08.029

[9] Corporate Headquarters, A123 Systems 2011, www.a123systems.com.

[10] Shenzhen Leadyo Technology Co., http://www.lifepo4-power.com.

[11] Grzesiak W, Maćków P, Maj T, Zawora S, Grzesiak P. Demonstrator of the charge controller, based on dedicated for stand-alone photovoltaic systems LiFePO4 technology; Przegląd Elektrotechniczny 2014; **9**: 29–32, DOI:10.12915/pe.2014.09.9

[12] Grzesiak W. The MPPT technique in charge controllers used in autonomous photovoltaic devices; Przegląd Elektrotechniczny 2010; **86**(11A): 187–189.

[13] Grzesiak W, Ciez M, Maj T. Modeling and monitoring of autonomous photovoltaic installations for the needs of mobile measuring stations; Przegląd Elektrotechniczny 2011; **87**(9A): 172–175.

[14] Grzesiak W, Witek K, Klugmann-Radziemska E. Microelectronics International 2014; 31(3, special issue): 224–228; DOI:10.1108/MI-11-2013-0071

[15] Grzesiak W, Maj T, Mackow P, Klugmann-Radziemska E, Zawora S, Grzesiak P. New solutions for the solar charge controllers design for obtaining true MPP in partly shaded PV modules; 29th European Photovoltaic Solar Energy Conference and Exhibition (EU PVSEC 2014), Amsterdam, 22–26 September 2014; pp. 3016–3019.

[16] Gibson TL, Kelly NA. Solar photovoltaic charging of lithium-ion batteries. Journal of Power Sources 2010; **195**: 3928–3932; DOI: 10.1016/j.jpowsour.2009.12.082.

[17] Grzesiak W, Guzdek P, Knapik R, Maćków P, Dzida W, Zawora S. The portable photovoltaic power generator, integrated with the collection and energy management system; application to the Polish Patent Office, No. P.410653.

Figure 1. Exemplary autonomous photovoltaic systems called ‘solar home stations’

Figure 2. Block diagram of the photovoltaic module integrated with the accumulator and innovative system for data gathering and power management

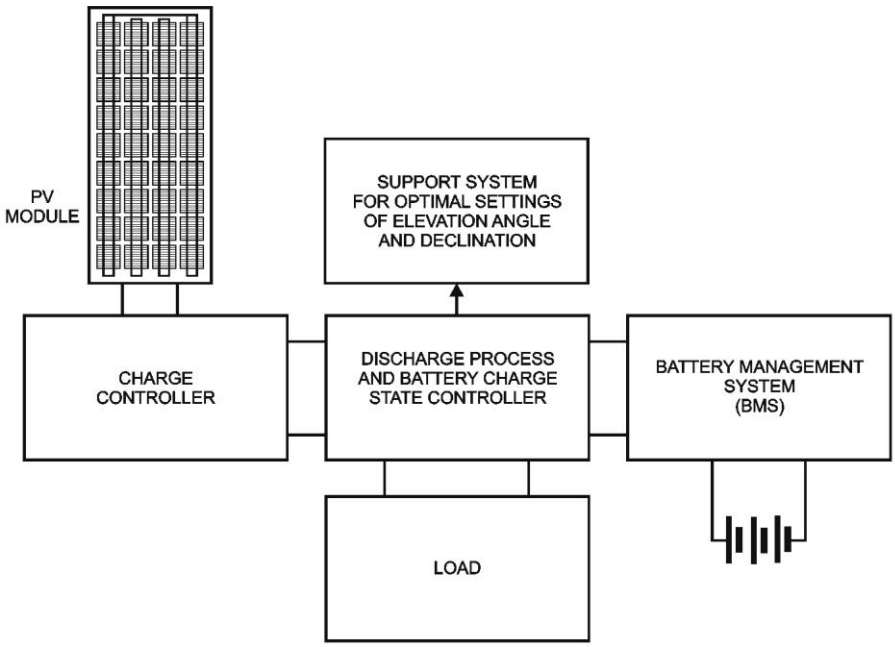

Figure 3. Details of the construction of the photovoltaic module integrated with the accumulator and innovative system for data gathering and power management

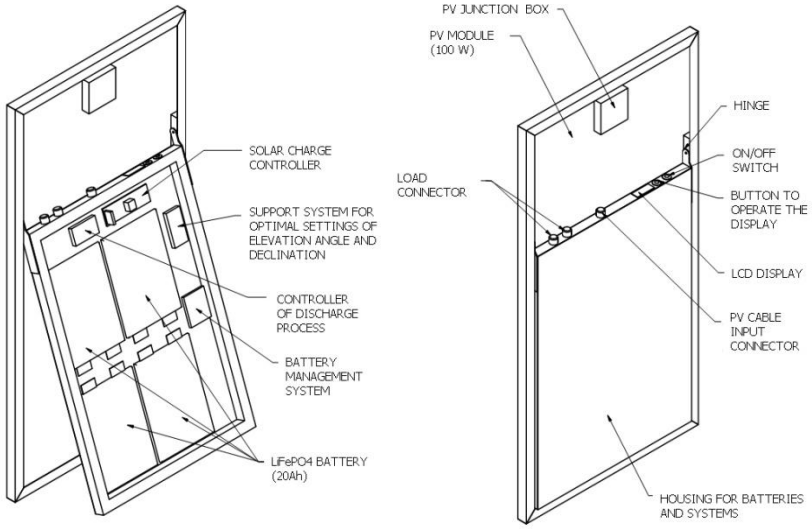

Figure 4. Schematic diagram of the battery charge controller

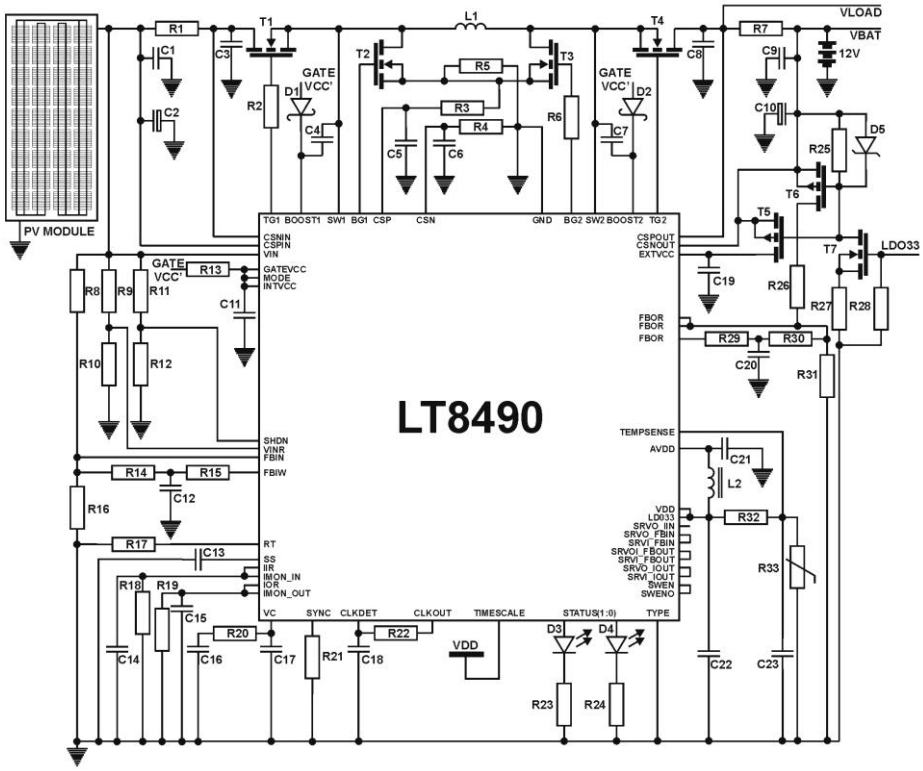

Figure 5. View of charge controller

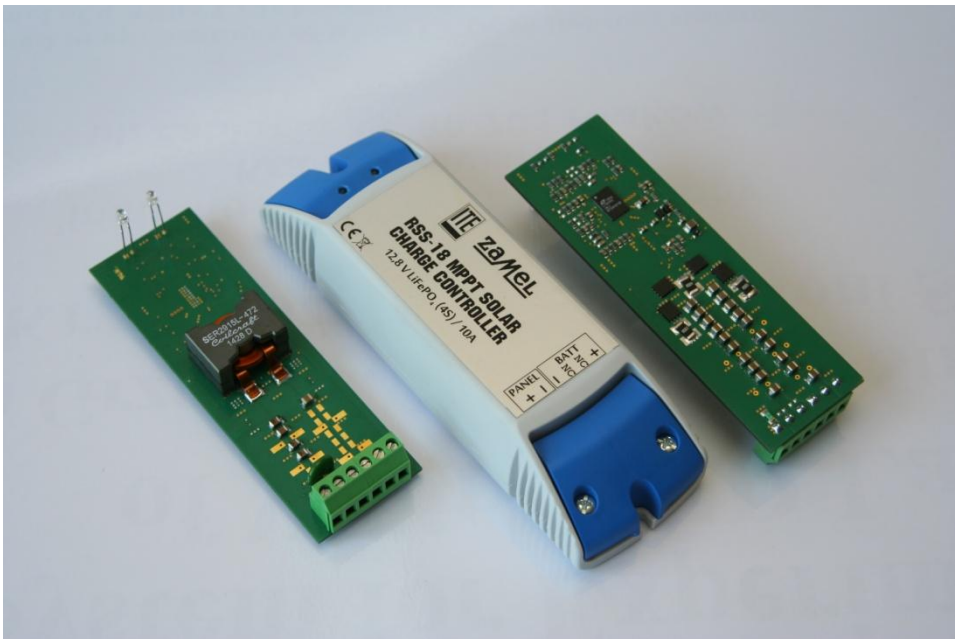

Figure 6. Schematic diagram of the battery discharge controller

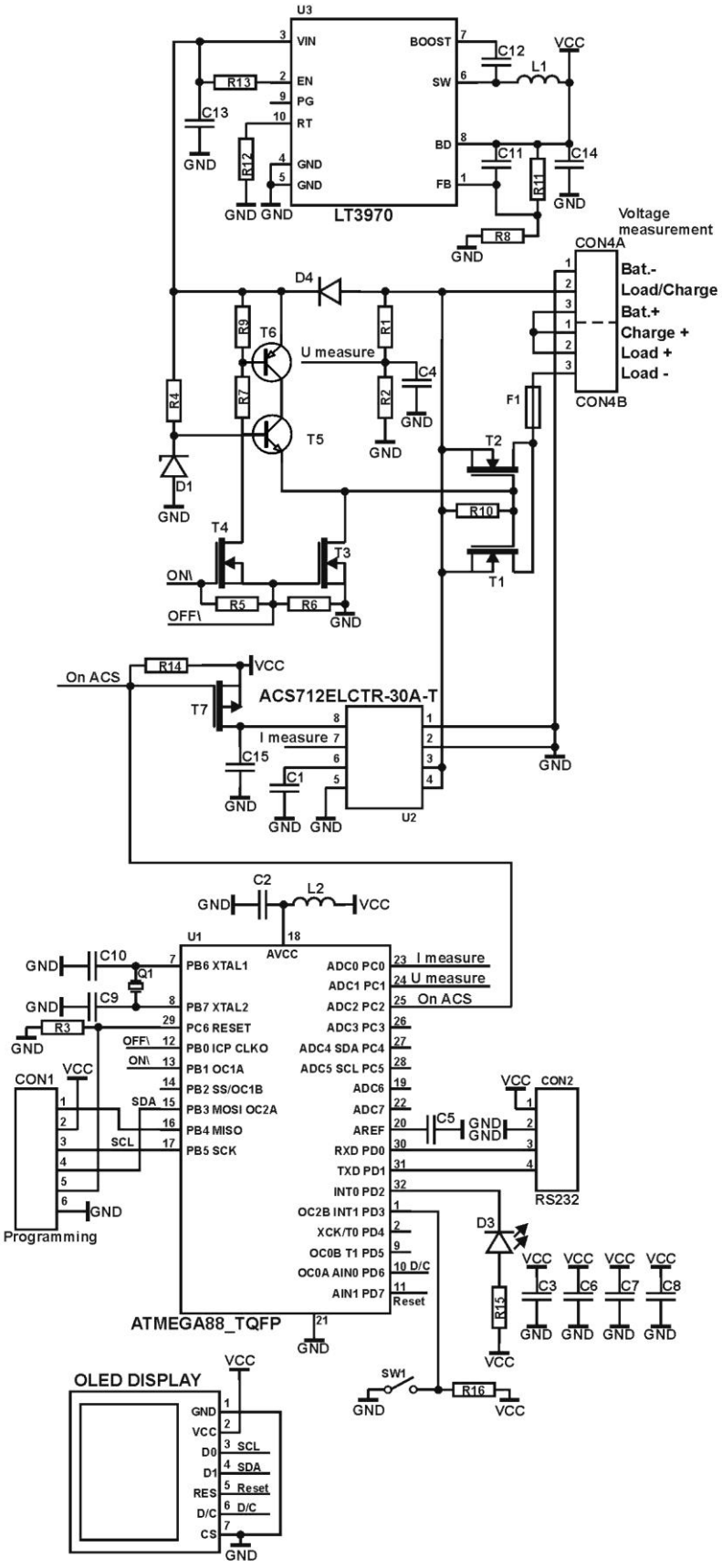

Figure 7. The manner in which the selected parameters are displayed

Figure 8. The scheme of the system for measuring the current-voltage characteristics of the module under different lighting conditions

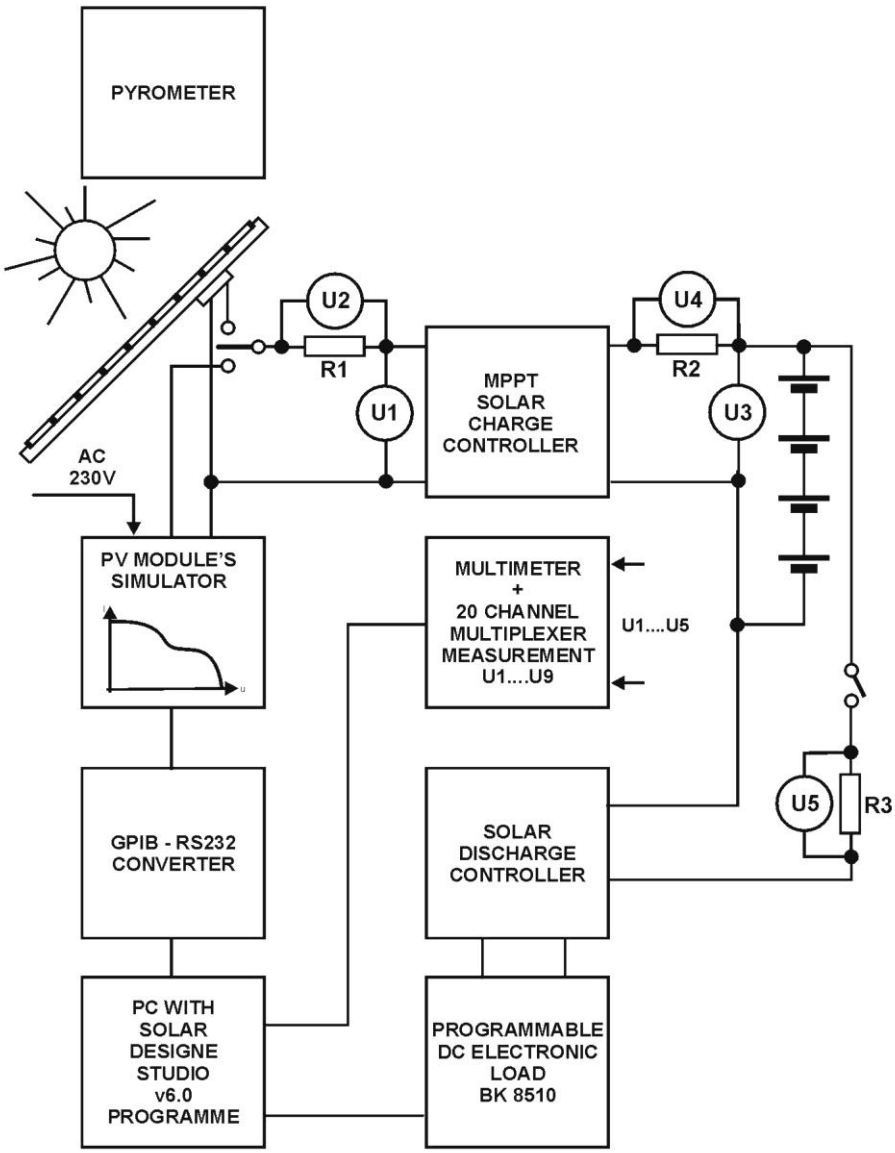

Figure 9. Exemplary characteristics of RS 36-125*125M-100 module

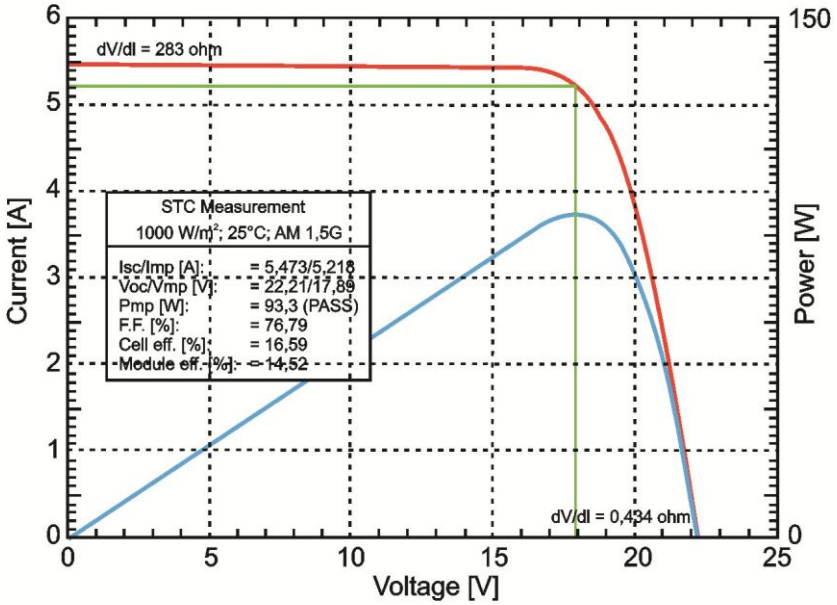

Figure 10. Current-voltage characteristics of the silicon monocrystalline module for irradiation of 200, 400, 600, 800, and 1000 W/m^2 and a temperature of 25 °C

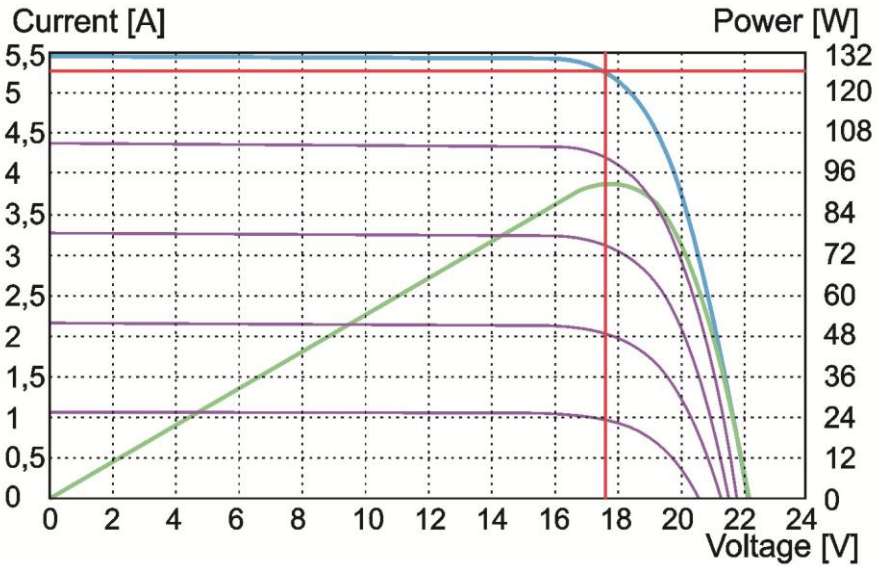

Figure 11. Characteristics of the partly shaded modules

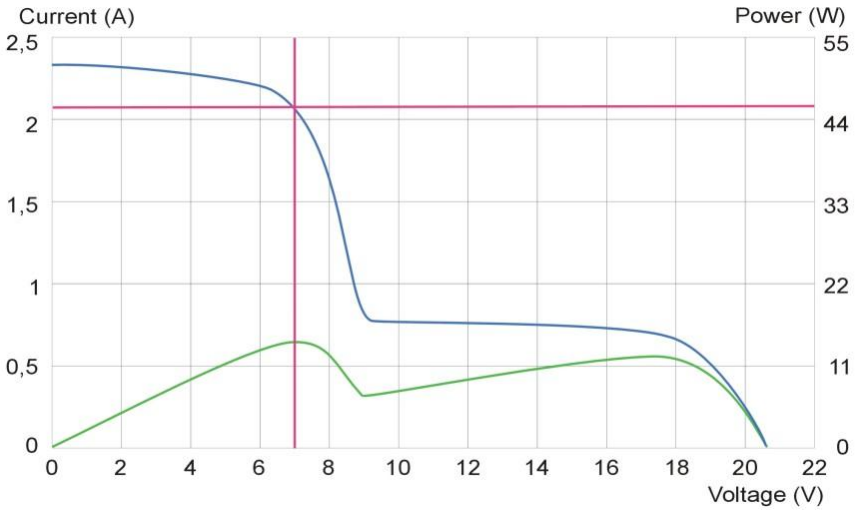

Figure 12. Dependency of the power generated by the SF 150/10A-155w module as a function of different shading configurations A–F

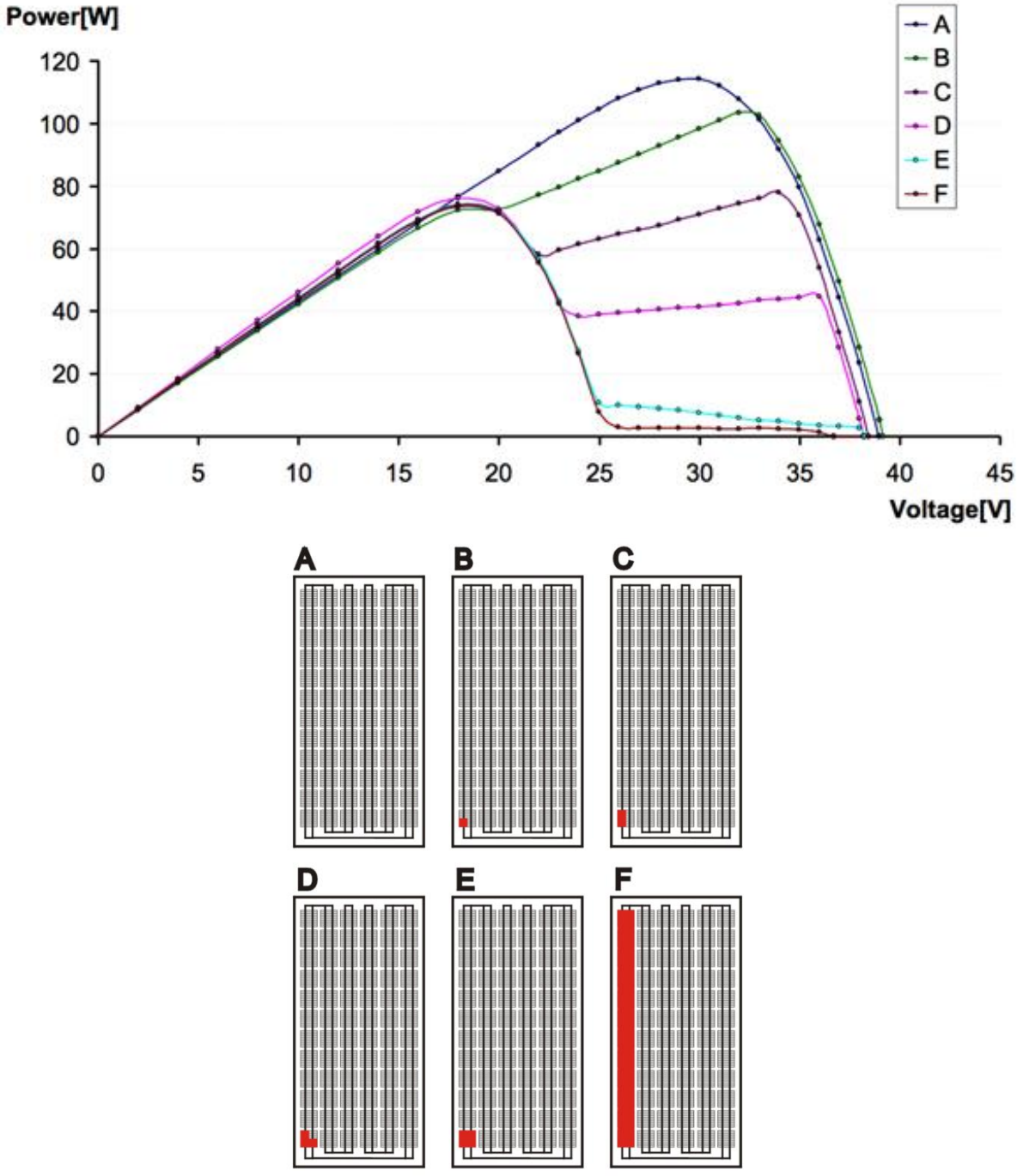

Figure 13. Characteristics of battery charging

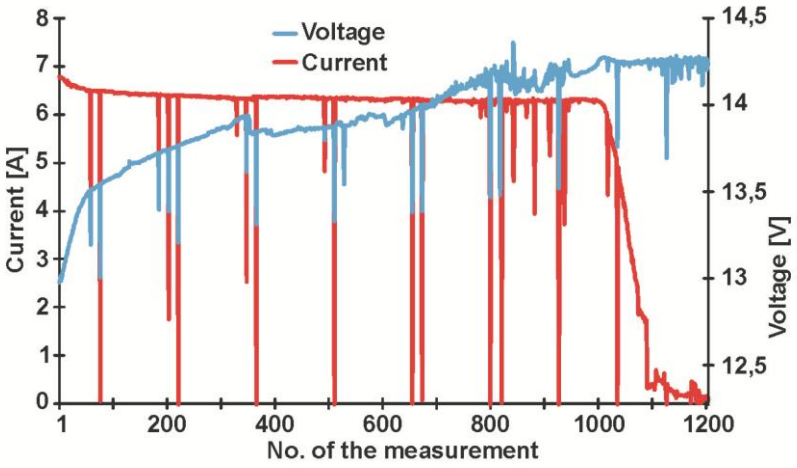

Figure 14. Discharge characteristics for the load currents of 5, 10, and 20 A

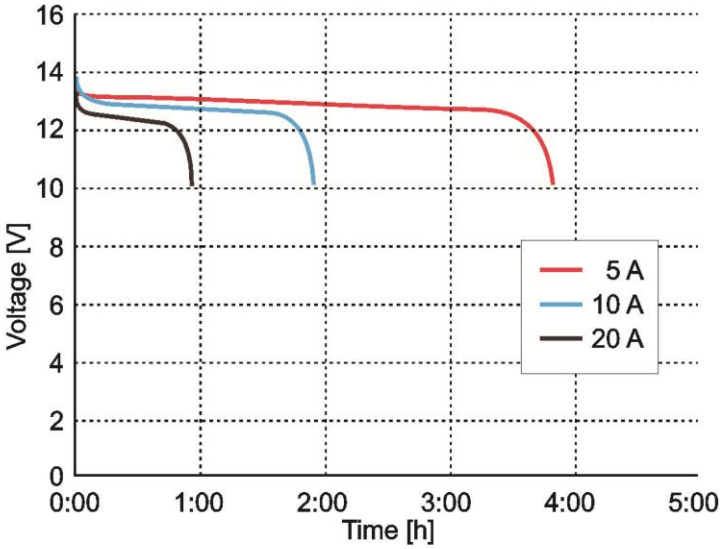

Figure 15. External view of the version with increased mobility